

# Pursuing prosthetic electronic skin

Alex Chortos<sup>1†</sup>, Jia Liu<sup>2†</sup> and Zhenan Bao<sup>2\*</sup>

**Skin plays an important role in mediating our interactions with the world. Recreating the properties of skin using electronic devices could have profound implications for prosthetics and medicine. The pursuit of artificial skin has inspired innovations in materials to imitate skin's unique characteristics, including mechanical durability and stretchability, biodegradability, and the ability to measure a diversity of complex sensations over large areas. New materials and fabrication strategies are being developed to make mechanically compliant and multifunctional skin-like electronics, and improve brain/machine interfaces that enable transmission of the skin's signals into the body. This Review will cover materials and devices designed for mimicking the skin's ability to sense and generate biomimetic signals.**

Skin plays a vital role in shaping our interactions with the world; we can effortlessly distinguish between a light breeze, a rough fabric and a smooth, hard surface. The ability to restore these capabilities to people with skin damage or amputations could provide an improvement in quality of life<sup>1,2</sup>. This ultimate scientific and engineering challenge motivates the development of a variety of new materials, devices and manufacturing methods. Active, robotic prosthetics can already mimic many of the mechanical properties of biological hands, and adding skin-like sensory capabilities could improve their acceptance and utility among amputees<sup>1,3</sup> by providing several key advantages. First, stimulating residual sensory pathways with sensory information can alleviate phantom limb pain that affects up to 80% of amputees<sup>4</sup>. Second, providing sensory feedback from a prosthetic limb provides the perception that the prosthetic is part of the user's body, promoting a sense of ownership<sup>3</sup>. Third, operating an active prosthetic based on visual and auditory cues can be cognitively straining<sup>1</sup>; providing tactile feedback could allow more natural and facile operation<sup>2,5</sup> by restoring information about body positioning (proprioception) and grip forces<sup>6</sup>. A lack of sensory feedback is currently a limiting factor for prosthetic devices<sup>1,5,7</sup>. According to consumers, design considerations for prosthetics include weight, cost, durability and life-like appearance<sup>8</sup>, and these requirements also apply to future prosthetic electronic skin.

## Biological inspiration

To restore a natural sense of touch, it is important to understand and mimic the key factors affecting the sensory properties of biological skin. The sensory receptors in human skin can be classified into seven general types: pain receptors, cold receptors, warm receptors and four mechanoreceptors that measure innocuous mechanical stimuli. The receptors encode information as the time between voltage spikes, called action potentials (Fig. 1a)<sup>9</sup>. Innocuous temperature is sensed by different afferents for cold and heat, covering the range from ~5 to 48 °C (refs 10,11). Each of the four types of mechanoreceptors (Fig. 1b) measures forces on different time-scales and with different receptive field sizes (Fig. 1c). The receptive field is the area of skin that elicits a response from the mechanoreceptor<sup>12–14</sup>. Slow adapting receptors (SA-I and SA-II) respond to static pressures; that is, they produce a sustained signal in response to a sustained stimulus. Fast adapting receptors (FA-I and FA-II) respond to dynamic forces (derivative of force with respect to time) and vibrations<sup>13,14</sup>. SA-I receptors are located near the surface of the

skin and respond to skin indentations with high sensitivity. They are in high densities in sensitive areas of the skin, such as the fingertips, and consequently provide high-resolution force information useful for discriminating object shape and texture<sup>15,16</sup>. SA-II receptors are located deeper within the skin and are primarily responsible for measuring skin stretch; therefore, they are important for proprioception<sup>13,14</sup>. FA-I receptors measure low-frequency (5–50 Hz; ref. 13) stimuli typically associated with object manipulation and texture discrimination<sup>15</sup>. They are essential for measuring the changing position of objects in a person's hand and for detecting slip that is used to adjust grip force<sup>6,13</sup>. FA-II receptors measure high-frequency vibrations (up to 400 Hz; ref. 13) over large areas, and are important for texture discrimination<sup>15,17</sup> and slip detection<sup>6</sup>. The signals from receptors are transported through nerve fibres, with each nerve fibre containing information from many receptors<sup>13</sup>. The ensemble output of information from these four receptors is interpreted by the brain to give complex information about body position and object size, shape, texture and hardness<sup>16</sup>. The time delay for the signal to reach the brain is in the range of several tens of milliseconds<sup>13,18</sup>.

The mechanical properties of skin have important effects on its sensory characteristics. Owing to its softness and compliance, skin adapts to the surface of an object, altering the distribution of forces on mechanoreceptors<sup>16</sup>, providing more contact area for sensory perception, and improving grasp through friction<sup>19</sup>. Mechanical structures within the skin, called intermediate ridges, may function to concentrate forces onto mechanoreceptors<sup>12</sup>, and fingerprint ridges on the surface of the skin are instrumental in texture discrimination<sup>17,19</sup>.

Additional sensing capabilities emerge as a result of the high density<sup>20</sup> and variety of sensors in the skin. For example, sensing large-scale textures is enabled by the large density of SA-I receptors<sup>14</sup>. The hardness of surfaces can be measured by the combined output of cutaneous receptors and proprioceptive receptors<sup>21</sup>, whereas the wetness of a surface is estimated based on sensations from both mechanoreceptors and thermal receptors<sup>22</sup>.

Skin has a unique combination of mechanical and sensory properties that do not exist in conventional electronics. Consequently, mimicking skin inspires the development of new materials and processing methods<sup>23</sup>. The components of skin that need to be developed include sensors, signal encoding, signal transmission and a method to convey the sensory information into the nervous system (Fig. 1d).

<sup>1</sup>Department of Materials Science and Engineering, Stanford University, Stanford, California 94305, USA. <sup>2</sup>Department of Chemical Engineering, Stanford University, Stanford, California 94305, USA. <sup>†</sup>These authors contributed equally to this work. \*e-mail: zbao@stanford.edu

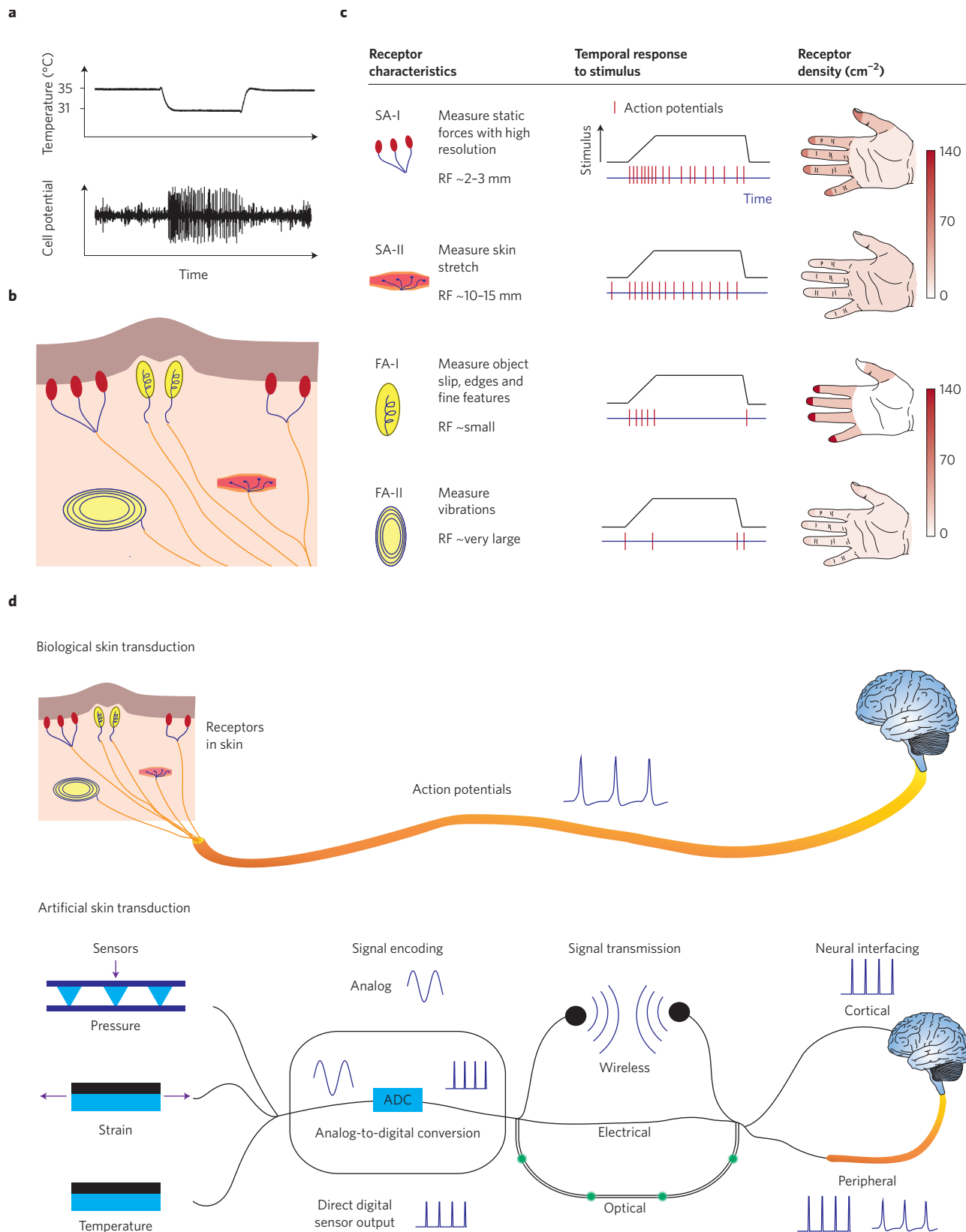


**Figure 1 | Skin receptors and transduction process.** **a**, Action potentials produced by cold receptors in human skin<sup>9</sup>. **b**, A schematic of the location of mechanoreceptors in the skin<sup>14</sup>. **c**, Types of mechanoreceptors, their function, temporal response and density in the hand<sup>13</sup>. RF, receptive field size; SA-I and SA-II, slow adapting receptors; FA-I and FA-II, fast adapting receptors. **d**, A schematic of the steps required for the transduction of sensory stimuli from natural (top) or artificial (bottom) receptors in the brain. Signal collection, encoding in electrical signals mimicking action potentials, transmission, and neural interfacing are all key issues that need to be addressed to add sensing capabilities to prosthetic devices. Figure adapted with permission from: **a**, ref. 9, Wiley; **b**, ref. 14, Elsevier; **c**, ref. 13, Nature Publishing Group.

### Mimicking mechanical properties

The skin's ability to accommodate the movements of the body by bending and stretching sharply contrasts with traditional silicon electronics that are rigid and brittle; alternative compliant electronics able to mimic and adapt to the skin are required for such applications<sup>23–25</sup>. Prosthesis consumers value skin-like coverings for their prosthetic devices that have a similar look and feel as real skin as well as good durability<sup>8</sup>. It has been shown that, by tuning the modulus, viscoelasticity and temperature of a skin-like coating, the touch from a prosthetic hand can be indistinguishable from a real hand<sup>26</sup>. Restoring both sensory feedback and the mechanical properties of natural skin may allow patients to comfortably use their devices during intimate interactions (for example, when interacting with children)<sup>7</sup>.

Flexible electronics<sup>27,28</sup> allow devices to be bent over curved surfaces such as fingers and provide some additional degrees of movement compared with rigid devices. In addition to favourable mechanical properties, using flexible substrates can facilitate advantageous processing methods, such as roll-to-roll processing or printing, that could reduce fabrication costs<sup>27,29</sup>. Considering that skin is the largest organ of the body, minimizing the per-area cost of its artificial replica will be a priority. Flexible electronics technologies such as polymer microelectromechanical systems<sup>27,30</sup> and thin-film transistor matrices are rapidly being developed<sup>31,32</sup>. Moreover, many traditional electronic devices can be made flexible by reducing the thickness of the substrate to reduce strains on the active materials<sup>33</sup>.

Flexible electronics technologies can satisfy many of the requirements for prosthetic electronic skin development<sup>24</sup>. However, to fully mimic the feel and sensory properties of skin, it is important to implement materials with low elastic moduli and good stretchability<sup>26</sup>. On average, biological skin is stretchable to 75% strain<sup>34</sup>, and this allows free movement of the joints, which experience surface strains up to 55% for the knees<sup>35</sup>. Furthermore, coverings for prosthetics that mimic skin mechanics to make the device appear and feel more natural are popular among prosthetics users<sup>26</sup>. Making electronics stretchable requires new materials or fabrication approaches that provide additional degrees of movement. We will discuss three major approaches to stretchable electronics: (1) buckling of flexible devices, (2) discontinuous stiff components and (3) intrinsically stretchable materials.

**Buckling.** In these approaches, a flexible device is attached to a pre-stretched elastomer substrate. When the substrate strain is released, the flexible device buckles out of the plane of the deformation (Fig. 2a). The substrate can then be stretched to the value of the original pre-strain by changing the radius of curvature of the electronic device; in other words, the buckling approach converts substrate stretch into bending of the active device. If the flexible device consists of a thin active material on a thicker substrate, the strain in the active material can be approximated by  $t/2r$ , where  $t$  is the thickness of the substrate and  $r$  is the radius of curvature<sup>36</sup>. Furthermore, by adding an encapsulation layer to the device, the active components can be positioned at the neutral mechanical plane<sup>25,37</sup>, which is the location of minimal strain in the device stack. Buckling approaches can be applied to any flexible device; hence, in principle, they can be used to convert any high-performance flexible electronic device into a stretchable one. However, some flexible sensors may change their sensing properties when bent<sup>38</sup>. Additionally, buckling may prevent the device from intimate contact with the target object.

**Discontinuous stiff components.** Stretchable electronics can be fabricated by patterning discontinuous stiff components in a softer substrate, so that the deformation is accommodated by the stretchable regions between the stiff islands (Fig. 2b). Electrical connections between stiff device islands can be formed by stiff non-stretchable materials that are designed to deform out of the plane of

deformation<sup>39</sup> or by intrinsically stretchable conductors<sup>40</sup>. For example, serpentine gold or silicon interconnects have been designed that bend in the  $z$  direction to accommodate strain applied in the  $x$  and  $y$  directions<sup>39</sup>. Intrinsically stretchable carbon nanotube-based inks have been developed to connect stiff islands made of polyimide<sup>40</sup>. The stiff island approach allows the use of high-performance rigid devices. However, the stretchability depends on the surface ratio between the stretchable interconnects and the rigid islands; hence, a trade-off between stretchability and device density is unavoidable.

**Intrinsically stretchable materials.** The development of intrinsically stretchable electronics has been challenging due to the need to create new materials with suitable mechanical and electronic properties<sup>41,42</sup>. Examples of such materials include composites in which electronic functionality is imparted to insulating elastomers by blending them with electronically active components<sup>40,43</sup>. In blended materials, higher filler content increases conductivity but reduces the stretchability. High-aspect ratio fillers simultaneously improve stretchability and conductivity by reducing the percolation threshold<sup>43</sup>. Two-dimensional networks of 1D materials, such as carbon nanotubes (CNTs) and nanowires, have excellent stretchability because the 1D materials can slide or deform while maintaining a percolating pathway<sup>44</sup>. The adhesion of the fillers in the network has a large effect on stretchability. CNTs tend to slip and buckle under strain, resulting in irreversible strain-induced changes that allow the device to be preconditioned, using an initial strain cycle, to have strain-independent characteristics within the preconditioned strain range<sup>44,45</sup>. In contrast, when nanowires are well adhered in a matrix, the electrical behaviour with strain is reversible<sup>46</sup>.

An alternative approach to adding electronic functionality to stretchable and insulating materials is to make electronic materials more mechanically compliant. Polymeric electronic materials have conjugated structures that typically promote crystal formation and brittle mechanical properties. However, by modifying the chemistry of the polymers and including additives, materials can be developed that have a favourable trade-off between mechanical compliance and electronic properties<sup>47,48</sup>.

Many of the individual components for prosthetic skin, including temperature sensors<sup>49</sup>, tactile sensors<sup>35,50–52</sup> and transistors<sup>45,53,54</sup>, have been demonstrated using intrinsically stretchable electronic materials (Fig. 2c). However, the fabrication processes and the device performance are not yet sufficient for the types of circuits required to process biomimetic signals, as discussed in the 'Methods for encoding biomimetic data' section. For instance, ionic dielectrics have dominated the field of stretchable transistors<sup>45,53,54</sup> because they are robust to thickness variations and are compatible with coplanar patterning methods<sup>54</sup>. However, ionic dielectrics often exhibit impaired time response and large hysteresis, limiting their applicability in prosthetic electronic skin.

**Toughness and durability.** Active prosthetics will be used in unstructured environments where they will be subjected to unexpected mechanical damage. Prosthetics users often find that skin-like coatings must be replaced regularly because of damage<sup>8</sup>. It is therefore clear that the toughness and durability of prosthetic electronic skin, the cost of which is expected to be higher than standard passive skin-like coverings, are mandatory conditions to enable the routine use of this technology. Elastomeric materials can sustain large pressures and impacts while remaining functional<sup>54</sup>, and choosing materials with high toughness and tear strength can ensure functionality despite punctures and tears<sup>45</sup> (Fig. 2d). Among elastomeric materials, there is often a trade-off between softness and durability; elastomers with skin-like elastic moduli often lack the durability required for prosthetics applications<sup>55</sup>. Real skin is both soft and tough because it is composed of a network of tough fibres, and these mechanical properties can

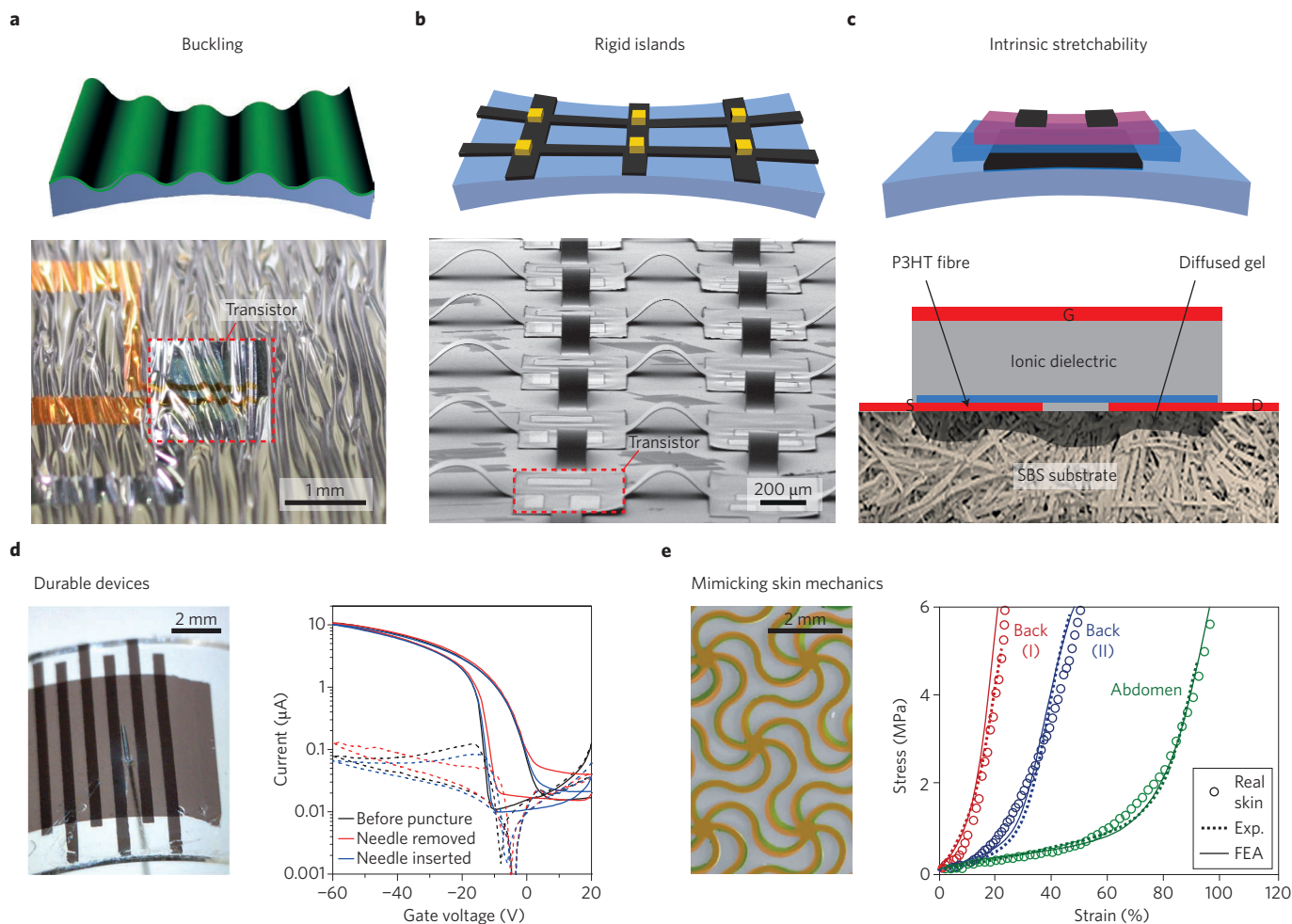


**Figure 2 | Strategies for imparting stretchability to electronic devices.** **a**, Substrate-level strategies include buckling<sup>33</sup>. **b**, Pixel-level approaches to stretchability involve connecting rigid device islands with stretchable interconnects<sup>39</sup>. **c**, Materials-level approaches involve the creation of devices using materials that are elastic<sup>53</sup>. P3HT, poly(3-hexylthiophene); SBS, styrene-butadiene-styrene. G, S and D represent the gate, source and drain electrodes. **d**, Highly durable and stretchable carbon nanotube transistors (left) that retain functionality despite impacts and punctures. Right: transistor transfer curve before and after inserting a needle into the channel<sup>45</sup>. Dashed lines represent the gate current, commonly referred to as leakage current. **e**, Substrates that use deterministic design (left) to mimic the mechanical properties of skin (right)<sup>56</sup>. The biomechanical properties of real skin at two locations on the back and one on the abdomen (open circles) are compared with experimental data (Exp.) for the bioinspired designs and finite element analysis (FEA) simulations of the deformation mechanics. Figure reproduced with permission from: **a,e**, refs 33,56, Nature Publishing Group; **b**, ref. 39, PNAS; **c,d**, refs 53,45, Wiley.

be mimicked by including a network of high-modulus materials within a network of low-modulus materials. The resulting composite has a very low modulus at low strains, whereas the modulus increases rapidly at higher strains to prevent rupture under large stresses, similar to the properties of real skin<sup>56</sup> (Fig. 2e). This allows the skin to be soft at low strains to enable a life-like feel and favourable grasp characteristics, whereas the toughness at larger strains prevents rupture.

### Recreating skin sensations

Skin detects a wide range of sensations, including temperature, pressure, strain and vibration. Below we describe methods for transducing these stimuli into electrical signals. Transduction is the first step in creating an artificial system that mimics the electrical output of biological receptors. A sensitive transducer and a signal-processing circuit are the key components of a biomimetic receptor, as discussed in ‘Methods for encoding biomimetic data’.

**Temperature transduction.** Biological thermoreceptors respond to static temperatures with relatively low sensitivity in the range of 1–14 Hz °C<sup>-1</sup> (refs 11,57), whereas the dynamic sensitivity is much

higher<sup>57</sup> (up to 70 Hz °C<sup>-1</sup>; ref. 11). Consequently, humans have limited ability to discriminate constant temperatures, but can identify temperature changes as small as 0.02 °C (ref. 57).

Temperature sensors for electronic skin (e-skin) have been demonstrated based on resistance thermometers, p–n junctions or composite materials undergoing thermal expansion. Resistance thermometers with linear temperature coefficient of resistance (TCR) have been used to measure the thermal properties of skin with a resolution of 0.014 °C (ref. 58). However, their sensitivity is low (<1% °C<sup>-1</sup>) and the sensing mechanism is strain-sensitive, so stretchability must be imparted using buckling or rigid island approaches<sup>33,58</sup>. The thermal sensitivity of p–n junctions is based on the thermal activation of charge carriers<sup>58,59</sup>. Although these devices have improved sensitivity compared with TCR sensors, they are also sensitive to light<sup>60</sup>. Highly sensitive devices can be made from composites based on a polymer matrix and a conducting filler<sup>49</sup>. As the temperature changes, thermal expansion causes the fillers to move apart, increasing the resistance<sup>60,61</sup> by up to six orders of magnitude with a resolution of 0.1 °C (ref. 60). These sensors often have large electrical hysteresis<sup>61</sup>, but they can be engineered to have minimal strain dependence<sup>49</sup>.

**Static force transduction.** Mimicking the function of SA-I receptors requires sensor arrays that can measure normal force distributions with a resolution of  $\sim 0.5$  mm (refs 12,23). SA-I receptors have a limit of detection  $< 1$  mN (ref. 62), their response includes both static and dynamic components<sup>63</sup>, and the sensing properties are highly dependent on strain rate<sup>64</sup>. SA-I receptors exhibit a sensitivity to pressure of 2–10 Hz kPa<sup>-1</sup> (ref. 63) or a sensitivity to skin indentation of 30–160 Hz mm<sup>-1</sup> (ref. 64). Transducers for static pressure stimuli rely most commonly on capacitive and resistive mechanisms.

In capacitive sensors, capacitance is typically modified by changing the distance or overlap between two parallel plate electrodes (Fig. 3a, left, top). Capacitive sensors can have excellent sensitivity and linearity<sup>65,66</sup>, but must be shielded to reduce susceptibility to electromagnetic interference. The dielectric of a capacitive sensor can consist of a solid polymer<sup>44</sup>, a microstructured elastomer<sup>50,65</sup>, or an air gap<sup>66</sup>. Compared with a solid polymer film, microstructuring the dielectric polymer allows the dielectric to deform freely into void space, minimizing viscoelastic effects and therefore improving the time response and sensitivity<sup>65</sup> (Fig. 3a, right).

Resistive sensors can employ two mechanisms: intrinsic materials piezoresistivity and contact resistance between a rough or structured conductor and an electrode. In the first mechanism, applied pressure modifies the band structure of a semiconductor or the distribution of conductive fillers in a polymer composite<sup>23,67</sup> (Fig. 3a, left, middle). Piezoresistive polymer composites exhibit large hysteresis, large confounding temperature sensitivity, and poor pressure sensitivity<sup>23</sup>. To overcome these drawbacks, many recent reports on resistive sensors rely on contact resistance modulation (Fig. 3a, left, bottom). The change in contact resistance is caused by a change in contact area between a conductor and an electrode<sup>51,68</sup>. Contact resistance is not inherently sensitive to temperature; consequently, confounding temperature effects can be minimized<sup>68</sup>. Furthermore, since contact resistance is a surface effect, devices can be made very thin, which can improve flexibility<sup>69</sup> and stretchability<sup>51</sup> and reduce crosstalk between elements.

Many sensors have sensitivities that are comparable or better than human skin<sup>51,65,68,69</sup>. Compared with skin's detection threshold of 1 mN, capacitive and resistive sensors can measure forces smaller than 0.05 mN (ref. 70) and 0.08 mN (ref. 68). Compared with skin's time response of  $\sim 15$  ms, the response time of sensors can vary from  $\sim 100$  ms for bulk piezoresistance<sup>29,71</sup> to  $< 10$  ms and  $< 20$  ms for devices based on capacitance<sup>38</sup> and resistance<sup>69</sup>, respectively. The future challenges for device development include mimicking the adaptive characteristics of biological receptors<sup>63</sup> and improving integration with readout circuitry.

**Static strain transduction.** SA-II receptors principally measure skin strains<sup>14</sup>, which can be achieved using the same general mechanisms as static pressure sensors. Resistive strain sensors are typically based on two main mechanisms that are illustrated by the equation for resistance:  $R = \rho L / A$ , where  $\rho$  is resistivity,  $L$  is length and  $A$  is the cross-sectional area. The first mechanism is based on a change in geometry ( $L$  and  $A$ ). As the device is stretched, the length increases, and the area decreases due to the Poisson effect<sup>72</sup>. The second mechanism is based on a change in  $\rho$ , which can be caused either by a change in the band structure of a semiconductor<sup>73</sup>, or a change in the percolation pathways between conductive particles in a composite material<sup>23,74</sup>. Traditional strain sensors based on geometric piezoresistivity in metals or semiconductor piezoresistance in silicon are suitable for measuring small strains ( $< 1\%$ ), but can be incorporated in stretchable designs to enable large-strain measurement<sup>75</sup>. Intrinsically stretchable sensors to measure large strains are enabled by materials innovations such as microfluidic liquid metal channels<sup>76</sup> and percolating CNT networks<sup>35</sup>. Stretchable capacitors can measure strain due to the change in dielectric thickness and electrode area, and they are often also sensitive to pressure<sup>44,52</sup>. This

resembles the multifunctional sensing properties of SA-II receptors, which exhibit moderate pressure sensitivity<sup>14</sup>.

**Dynamic force transduction.** Piezoelectric and triboelectric sensors (Fig. 3b) produce a voltage in response to mechanical deformation. Deformation changes the magnitude of dipoles in the active layer, which causes a build-up of charge on the electrodes. In piezoelectric materials, dipoles originate at the molecular level. The application of strain to a material with a non-centrosymmetric unit cell can change either the magnitude of the dipole in the unit cell or the number of dipoles per volume of material<sup>77</sup>. This can occur in both inorganic materials, such as ZnO (ref. 78) and BaTiO<sub>3</sub> (ref. 79), and organic materials such as polyvinylidene fluoride. In triboelectric devices, macroscopic dipoles are induced by a process called contact electrification, in which charges are separated because of a difference in work function between two materials<sup>80</sup>. These sensors are selectively sensitive to dynamic pressures, making them suitable for mimicking the properties of FA-I and FA-II receptors<sup>12</sup>. Piezoelectric and triboelectric sensors have the additional advantage of producing energy during mechanical stimulation, enabling self-powered applications<sup>80</sup>. Forming piezoelectric materials into different structures can provide added functionality, such as high sensitivity<sup>81</sup> or stretchability<sup>82</sup>. Furthermore, vertical pillars can allow arrays<sup>78</sup> with densities much higher than FA-I receptors in biological skin.

**Biomimetic sensor arrays.** Several biomimetic strategies have been implemented to improve the performance of devices and provide more skin-like functionality. In biological skin, intermediate ridges act to concentrate forces onto SA-I receptors, and fingerprint ridges create friction to enable texture perception using FA receptors<sup>12,83</sup>. The structure of the intermediate ridges has inspired approaches to concentrate forces in artificial systems to increase the sensitivity (Fig. 3c)<sup>83</sup>. Structures resembling fingerprint ridges have been used to facilitate texture perception by inducing vibrations<sup>83</sup> and allow the discrimination of shear forces<sup>84</sup>.

Receptors in biological skin are embedded at different depths to tune their sensitivity to stimuli<sup>14</sup>. Receptors located near the surface of the skin (similar to SA-I receptors) are more sensitive to pressure stimuli, whereas receptors located deeper in the skin (similar to SA-II receptors) are more selective for stretching stimuli<sup>76</sup>. Similarly, embedding receptors at different depths in artificial skin helps to understand complex force distributions (Fig. 3d)<sup>85</sup> and to tune the sensitivity of receptors to different stimuli<sup>76</sup>. It is common to add an elastomeric coating to pressure sensor arrays<sup>86</sup> to increase friction for grasping tasks. Like in biological skin, this elastomeric coating also affects force distributions and increases hysteresis<sup>87</sup>.

Sensing the complex range of mechanical and thermal stimuli in skin requires multiple types of sensors. These different stimuli should be individually resolved<sup>88</sup>, similar to biological skin in which there are selective sensors for skin sensations such as temperature and vibration. Multilayer artificial skins have been developed that sense multiple sensations (Fig. 3e and Table 1). Measuring multiple stimuli using a single transducer can alleviate space constraints. However, to distinguish multiple stimuli, the device must include more than two terminals and include either comparative calculations<sup>50,84</sup> or a biasing scheme that produces multiple measurable outputs<sup>79</sup>. Artificial skins have also incorporated dedicated sensors for properties such as humidity<sup>75,89</sup> that, in human skin, are instead estimated using combinations of receptors<sup>21,22</sup>. It is currently unclear how the body would interpret information from sensors that are not typically found in skin.

### Methods for encoding biomimetic data

For safe and effective stimulation of nerve tissue, pulse-like waveforms mimicking action potentials are employed. The amplitude, frequency and duration of the stimulus pulses are among the most important parameters<sup>90</sup>. To directly interface electronic skins with

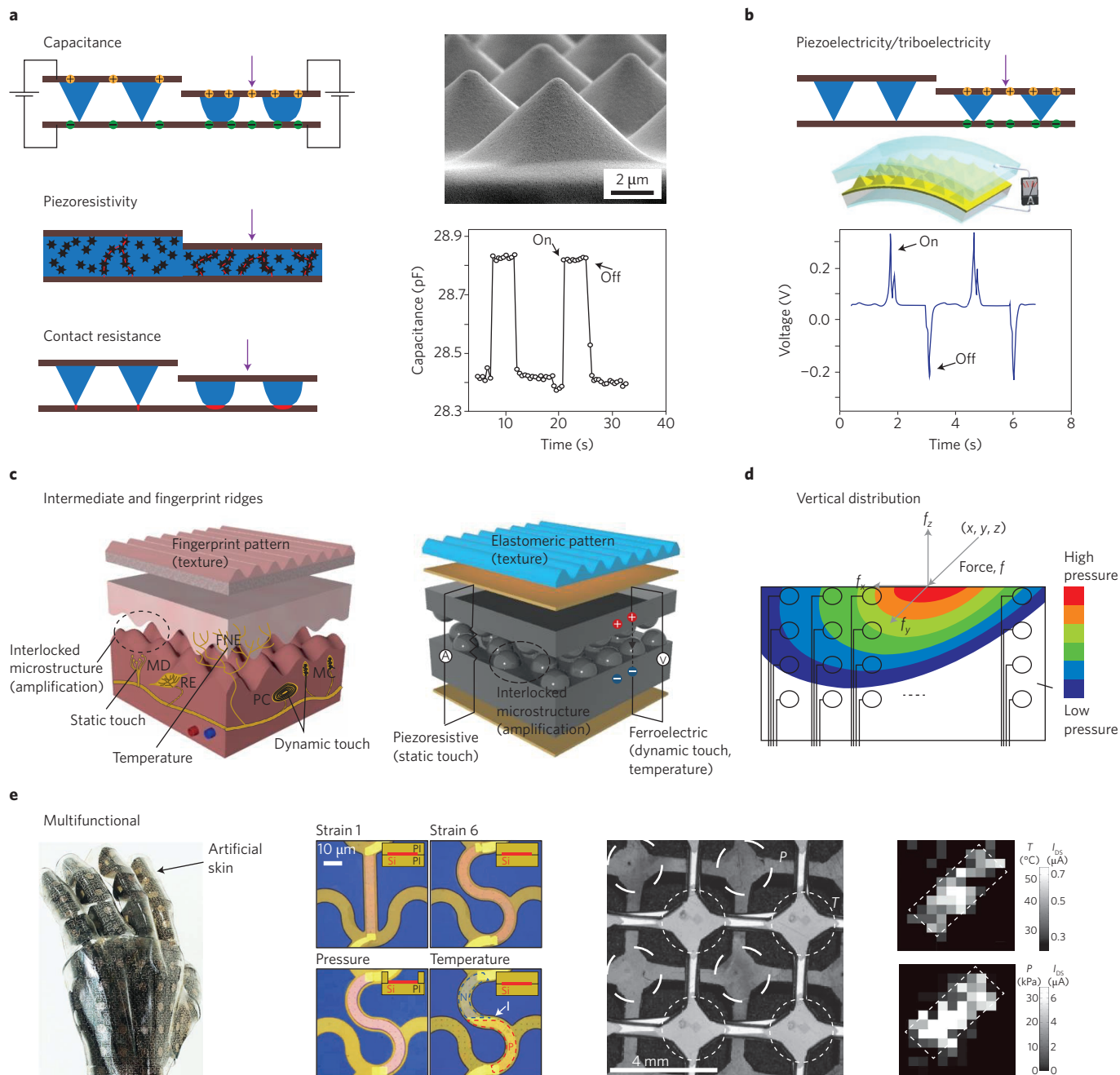


**Figure 3 | Devices for transducing sensory stimuli in skin.** **a**, Left: capacitive (top), bulk piezoresistance (middle), and contact resistance (bottom) mechanisms for measuring static pressure. Purple arrows indicate applied pressure; black stars indicate conductive fillers and red dashed lines indicate percolation pathways (middle); red highlights indicate the size of the contact area (bottom). Right: a capacitive sensor with a pyramid-structured dielectric (top) showing constant response with constant pressure (bottom)<sup>65</sup>. **b**, Triboelectric and piezoelectric devices produce a voltage in response to pressure (top). A flexible triboelectric device (middle) with dynamic response to pressure stimuli (bottom)<sup>127</sup> that could fulfil the role of FA-I and FA-II receptors. **c**, Intermediate ridges can be used to concentrate force, and fingerprint patterns can help distinguish texture<sup>83</sup>. FNE, free nerve endings; MD, Merkel disks; RE, Ruffini corpuscles; PC, Pacinian corpuscles; MC, Meissner's corpuscles. **d**, Four vertically separated layers of pressure sensors can be used to understand complex force distributions<sup>85</sup> in the same way as biological skin. **e**, Left panels: multifunctional e-skins include devices based on silicon nanoribbons that can measure strain, pressure ( $P$ ), temperature ( $T$ ) and humidity<sup>75</sup>. N, P and I represent n-type, p-type and intrinsic regions of the Si ribbon, respectively. Right panels: a multilayer organic active matrix to measure pressure and temperature<sup>59</sup>.  $I_{DS}$ , source-drain current. Figure reproduced with permission from: **a,e** (left panels), refs 65,75, Nature Publishing Group; **b**, ref. 127, American Chemical Society; **c**, ref. 83, AAAS; **d**, ref. 85, IEEE; **e** (right panels), ref. 59, PNAS.

nervous systems, the electrical output from sensors need to be modified in a way that their parameters can be intelligible to nervous systems. Recently demonstrated flexible electronics technologies include the key components that can be used for this signal modification process to encode biomimetic signals for further neuron

modulations. In addition, to restore proprioceptive sensation, high-density sensor arrays need to be implemented into electronic skin to cover a sufficiently large area while maintaining a high spatio-temporal resolution; as a result, flexible readout matrices are also important for enabling an efficient data sampling and transmission.

**Table 1 | Summary of selected demonstrations of electronic skin compared with human skin.**

Technology	Sensor density (cm <sup>-2</sup> )					Electrical output	Multiplexing	Mechanics
	T	P	S	D	H			
Human fingertips <sup>20</sup>	4	70	48	163*	-	Digital	Direct address	Stretchable, durable, self-healing, biodegradable
Human palm <sup>20</sup>	4	8	16	34*	-	-	-	-
Stretchable carbon nanotubes <sup>44</sup>	-	25	-	-	-	Analog	Passive matrix	Stretchable
Self-healing sensor <sup>67</sup>	-	1	-	-	-	Analog	-	Self-healing
Biodegradable polymer <sup>70</sup>	-	13	-	-	-	Analog	Passive matrix	Biodegradable
Stretchable silicon <sup>75</sup>	11	44	44	-	1	Analog	Passive matrix	Stretchable
Piezotronic <sup>78</sup>	-	8,464	-	-	-	Analog	Passive matrix	Flexible
All-graphene <sup>89</sup>	25	25	-	-	25	Analog	Passive matrix	Stretchable
Carbon nanotube active matrix <sup>71</sup>	-	8.9	-	-	-	Analog	Active matrix	Flexible
Organic active matrix <sup>59</sup>	7.3	7.3	-	-	-	Analog	Active matrix	Flexible
Organic digital <sup>92</sup>	-	1	-	-	-	Digital	-	Flexible
POSFET <sup>123</sup>	-	-	-	100	-	Digital	Active matrix	Rigid silicon

The types of sensors are indicated by: T, temperature; P, pressure; S, strain; D, dynamic forces, H, humidity. POSFET = piezoelectric oxide semiconductor field-effect transistor<sup>26</sup>. \*Includes the added density of both FA-I and FA-II receptors.

**Circuits for encoding biomimetic output.** The magnitude of the stimulation pulses controls the sensation and the size of the perception area. To alter the amplitude of stimulation, an amplifier could amplify the signal recorded from the sensor array (Fig. 4a,b). Flexible amplifiers have been realized by different methods, such as transferring a silicon membrane or patterning organic semiconductors<sup>32,37,91</sup> on flexible substrates and connecting them into established complementary metal-oxide semiconductor (CMOS) architectures. The intensity of sensation is influenced by the frequency of stimulation. To convert the analog signals recorded from sensors into digitized frequency signals, the amplified signal from the sensor can be used to modulate the frequency of a ring oscillator. Flexible printed complementary organic ring oscillators have been used to optogenetically stimulate the brains of mice<sup>92</sup>.

Additional circuits are required to control the waveform of the stimulus. Charge balanced waveforms are important for electrical stimulation<sup>93</sup>, whereas in optical stimulation, which is usually highly efficient, it is important to limit the stimulus duration. For example, an edge detector can be used to produce a specific pulse width compatible with optical stimulation<sup>92</sup> (Fig. 4c,d). The key electronic components required in these flexible circuits have already been demonstrated using silicon membranes<sup>37,91</sup> as well as flexible oxide and CNT devices<sup>31</sup>.

Finally, wireless powering and data transmission have been achieved through the use of flexible coils or by integrating radio-frequency data transmission modules on flexible and stretchable interconnects<sup>94,95</sup>, which could be adapted to the prosthetic electronic skin system. Using current flexible technologies, it is now possible to assemble the components necessary to produce digital signals for neural modulation into a closed-loop system, which could record, convert and transmit the signals from sensors into the nerve tissue.

**Sensor integration with readout electronics.** To realize fully biomimetic skins, sensor arrays with multiple functions need to cover large areas with high density, enabling high spatiotemporal resolution. However, reducing the size of sensors reduces the amplitude of analog signals such as capacitance or current, and increasing the density of sensors and interconnect lines results in increased crosstalk. These problems can be addressed by combining each sensor with a transistor to provide local signal transduction and amplification. Furthermore, transistor integration facilitates multiplexing (using an active matrix), which can reduce the number of required sampling

lines<sup>40</sup>. Compared with passive matrix addressing, there is also significant power saving using an active matrix scheme. Capacitive sensors or piezoelectric sensors can be integrated as the gate dielectric in a transistor<sup>38,79,88</sup> (Fig. 5a) or along a gate electrode that extends out from the device. Resistive sensors have often been incorporated in the source of a transistor to facilitate multiplexing<sup>29,40</sup> (Fig. 5b).

Digitizing the signal at the site of sensation reduces the effects of interference along the signal propagation pathway. Integrating the sensor with an analog-to-digital (A/D) converter, such as a ring oscillator (Fig. 5c), can enable the direct conversion of a sensory signal into a digital signal without the need for an amplifier or external A/D converter<sup>92</sup>. To tune the shape of the stimulus-response curve, the sensor and system can be co-optimized<sup>96</sup>. For example, sensors based on the variation of contact resistance of a random interface have power-law stimulus-response relationships<sup>68</sup>, but other shapes can be obtained by controlling the contact properties of the interface<sup>51</sup>. In ref. 92, the exponential signal from a resistive sensor was converted to a biomimetic frequency output by integrating the sensor as a voltage divider with an oscillator (Fig. 5c).

There are a number of strategies to read out information from arrays of sensors. An active matrix of sensors could be combined with an external A/D converter (Fig. 5d, left). Although this method does not facilitate event-driven sensing, it allows a high density of sensors and is more compatible with inputting signals into the central nervous system (CNS). Alternatively, the analog signal can be locally transduced by an A/D converter<sup>92</sup> (Fig. 5d, middle), and the resulting biomimetic signal could directly stimulate the peripheral fibres that connect to the target afferent. This method retains biomimetic characteristics such as low power and event-driven sensing. A third option is to connect the digital outputs from multiple locally digitized sensors along the same sampling lines (Fig. 5d, right). In this case, the signals must be distinguishable to encode the location of the stimulus.

### Restoring natural touch perception

Delivering the biomimetic signals described above to the nerve system is the last, important step to restore natural touch perceptions and proprioception with a prosthetic electronic skin; yet, it is very difficult due to the limited understanding of neural coding for perception and the challenge of building a stable and cell-specific electronics/nervous system interface. Stimulation of central and peripheral nervous systems has been achieved by electrodes<sup>97</sup>, optics<sup>98</sup>, acoustic induction<sup>99</sup> and electromagnetic inductions<sup>13,100</sup>.

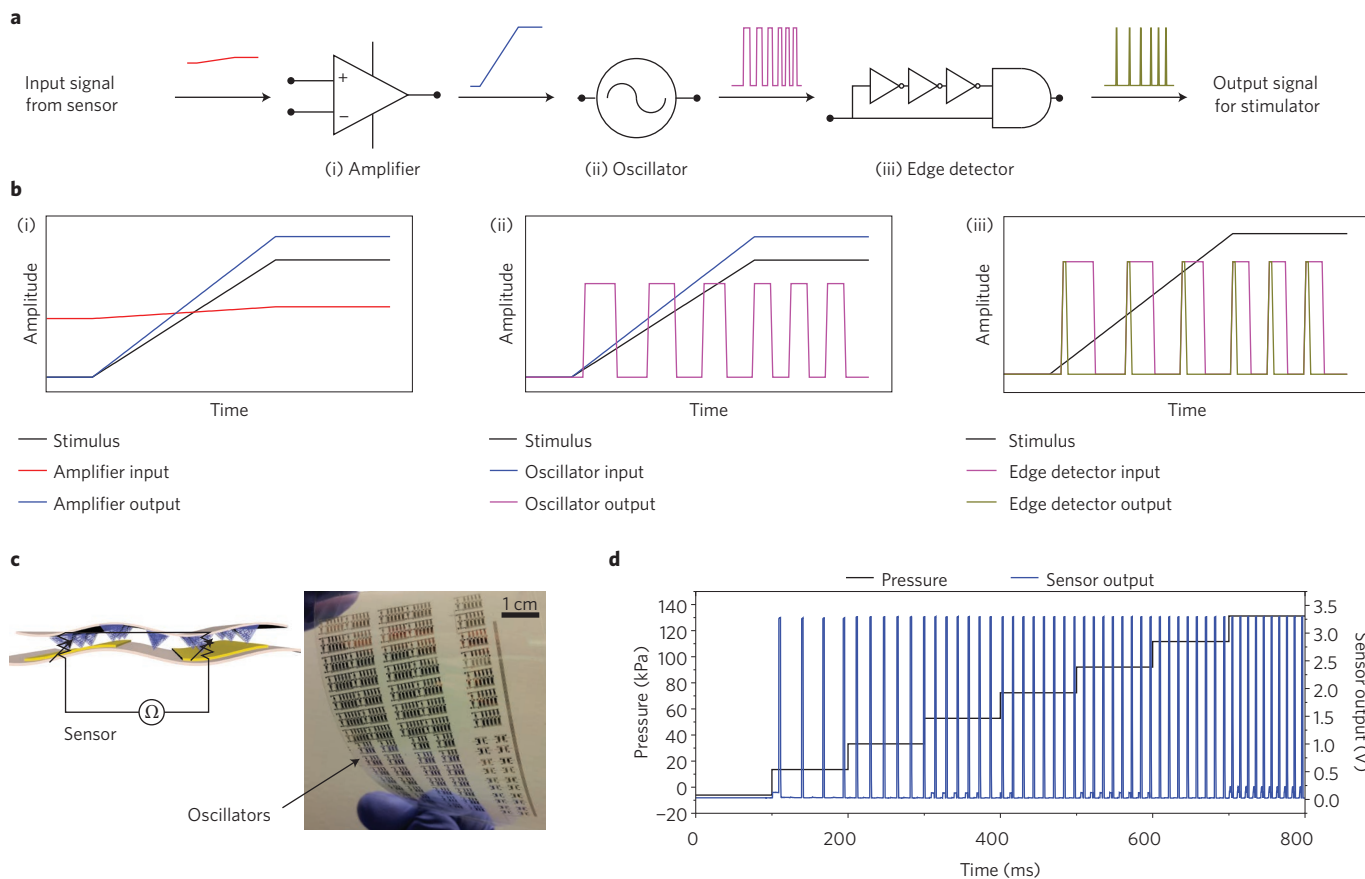


**Figure 4 | Readout electronics design that may be used for collecting and converting biomimetic data.** **a**, A schematic process for the conversion of the input signal into electrical spikes, requiring an amplifier (i), an oscillator (ii) and an edge detector (iii). **b**, Example data showing the input and output signals from each stage of the signal processing circuit. The input into the amplifier is an example sensor input, and the output from the edge detector is a biomimetic signal that encodes stimulus intensity as ‘action potentials’. **c**, Schematic of a resistive pressure sensor (left) and image of printed ring oscillators (right) used in an artificial mechanoreceptor<sup>92</sup>. **d**, Example output data from the mechanoreceptor components illustrated in panel **c** (ref. 92). Figure reproduced with permission from: **c,d**, ref. 92, AAAS.

We will mainly survey electrical, optical and magnetic stimulation methods, discussing the studies of these methods for restoring touch perception and the most advanced examples for implementing prosthetic electronic skin. Figure 6a–d illustrates some of the locations being used for the nerve interface, including somatosensory cortex, spinal cord, muscle tissue and peripheral nervous systems. Table 2 summarizes different interfacing methods for touch perception restoration. To fully exploit the advancements in sensors and circuits development described above for restoring touch perception and proprioception with spatiotemporal resolution comparable to natural skin, a more advanced bioelectronic interface is required to address the challenges of interfacing with a large number of neurons with cell-specific targeting capability. Figure 6e illustrates some of the emerging techniques that could be potentially combined with prosthetic electronic skins to realize multiplexed, cell-specific and long-term stable neural interfaces for perception restoration.

**Electrical stimulation.** For the CNS, direct intracortical micro-stimulation through the implanted electrode with natural somatosensory coding patterns could provide sensory feedback to body areas where patients still have somatosensation (Fig. 6a(i)). However, it is difficult to evoke constructive sensory percepts using this method, because of a limited control on the neural activation fields triggered by the electrical stimulation and because of the gradual degeneration of the interface between the invasive electrodes and the targeted brain region over a long period of time<sup>75,101,102</sup>. Afferent projections from the spinal grey matter also carry somatosensory and

proprioceptive information. Imaging studies with genetic labelling<sup>103</sup> have offered better strategies to illustrate the relative pattern between the mechanoreceptors and spinal cord, which can further provide a map for the somatosensory perception restoration through spinal cord stimulation. Therefore, epidural and subdural electrical stimulation could potentially be used for interfacing prosthetic electronic skin with the spinal cord (Fig. 6b(i))<sup>104</sup>.

Non-invasive stimulation of the reinnervated chest region with a dense electrode array could provide tactile sensation with precise somatotopic organization (Fig. 6c(i)). The challenge of this method is the limited spatial resolution of perception and lack of specificity, rapid fatigue of muscle fibres in a non-physiological order, and high voltage required for actuation due to the resistance of skin<sup>105</sup>.

Peripheral neurons are stimulated with simpler neuron codes and could provide parallel information to the brain<sup>5</sup>. Peripheral nerve interfacing is less risky than direct brain tissue interfacing and has the highest chance for success. It is the most conservative approach for somatosensory interfacing even though it cannot benefit spinal cord-injured patients. Current electrical stimulation methods mainly exploit extra-fascicular and intra-fascicular electrodes to innervate peripheral nerves (Fig. 6d(i)). Extra-fascicular electrodes, such as cuff electrodes<sup>106</sup> and flat interface nerve electrodes<sup>107</sup>, have enabled some degree of specificity in the recruitment of peripheral nerve afferents. Since these electrodes do not penetrate into the nerve tissue, they cause less chronic damage<sup>91,108</sup> and have higher stability (versus intra-fascicular electrodes). However, due to the isolation from the protective sheath, high stimulation current



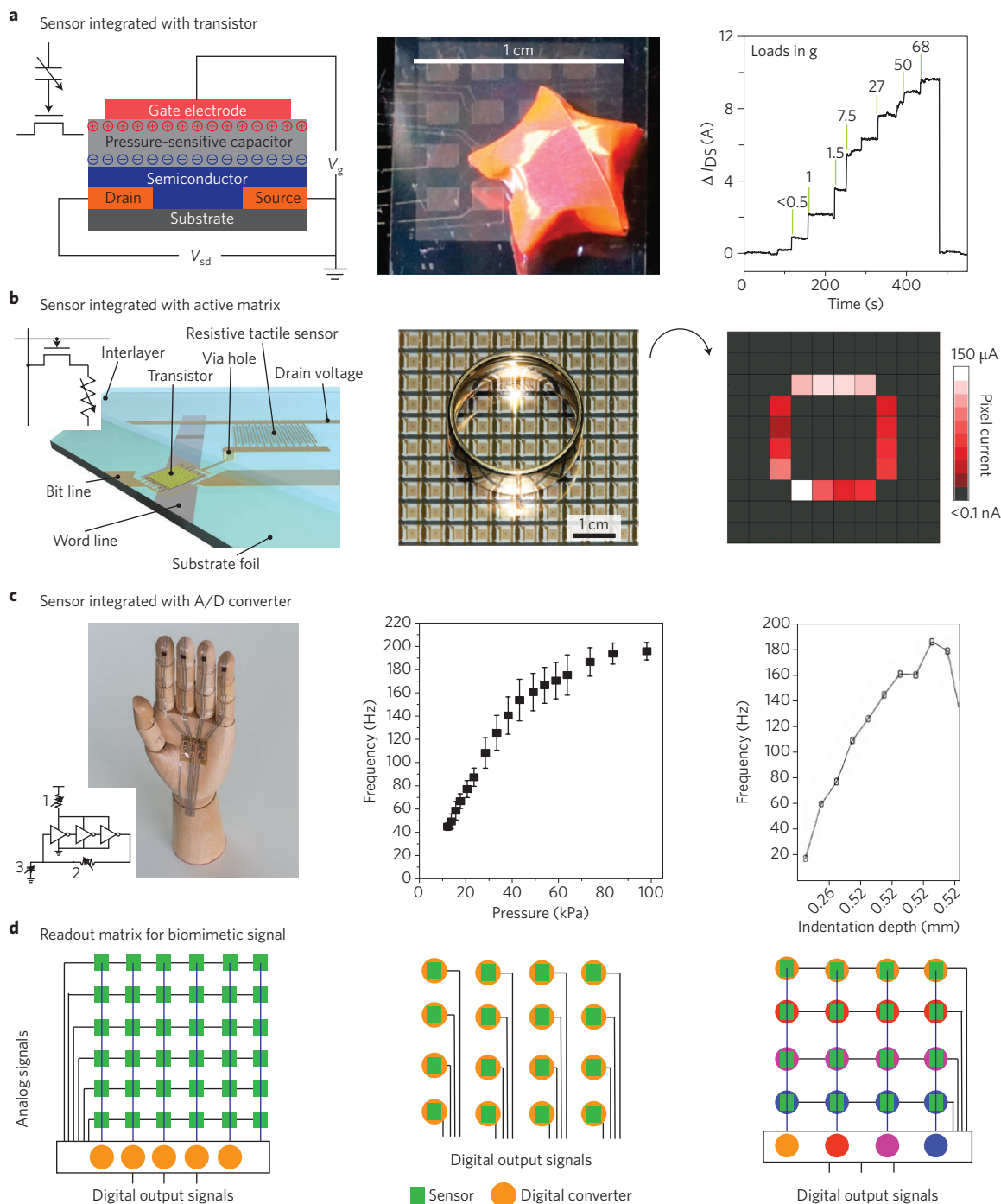


**Figure 5 | Sensor and circuit designs for signal readout and addressing.** **a**, A sensor integrated with a transistor for *in situ* signal transduction and amplification. Left: a schematic showing the device structure of a capacitive sensor integrated with a transistor. Inset: a circuit diagram of a sensor integrated with a transistor for signal transduction.  $V_{sd}$  and  $V_g$  represent the voltage applied between source and drain electrodes, and gate and drain electrodes of the transistor, respectively. Middle: 2D pressure mapping using a matrix of transistor-integrated sensors<sup>38</sup>. Right: representative performance of an organic transistor in response to pressure<sup>65</sup>.  $I_{DS}$  represents the current flow across the source and drain electrodes. **b**, Sensor array integrated with an on-site multiplexing circuit. Left: schematic showing the resistive sensor integrated with a switching transistor. Inset: circuit diagram of a sensor integrated with a transistor for multiplexing. Right: representative tactile sensing array used for mapping a metallic ring<sup>33</sup>. **c**, Sensor integrated with an analog-to-digital (A/D) converter to generate a biomimetic signal<sup>92</sup>. Left: image shows a model hand with pressure sensors on the fingertips connected with stretchable connectors to an A/D converter. Inset: schematic of integrating sensors with an oscillator. 1, 2 and 3 indicate the mechanisms through which the frequency can be modulated. 1, change supply voltage; 2, change resistance of feedback loop; 3, change capacitance of feedback loop. Middle: frequency output of the sensor-oscillator combination<sup>92</sup> compared with that of a real mechanoreceptor<sup>64</sup> (right). Error bars are one standard deviation based on 10 measurements of increasing pressure. **d**, Integration of a sensor array with a readout matrix. Left: schematic of an active readout matrix for collecting and converting analog signals from sensors. Middle: schematic of a passive readout matrix for collecting biomimetic and digitized signals converted by *in situ* A/D converters from each sensor. Right: schematic of an active readout matrix for collecting biomimetic and digitized signals. Different A/D converters will be used to generate output signals with encoded proprioceptive information. Figure reproduced with permission from: **a** (middle), **a** (right), **b**, refs 38,65,33, Nature Publishing Group; **c** (left, middle), ref. 92, AAAS; **c** (right), ref. 64, Society for Neuroscience.

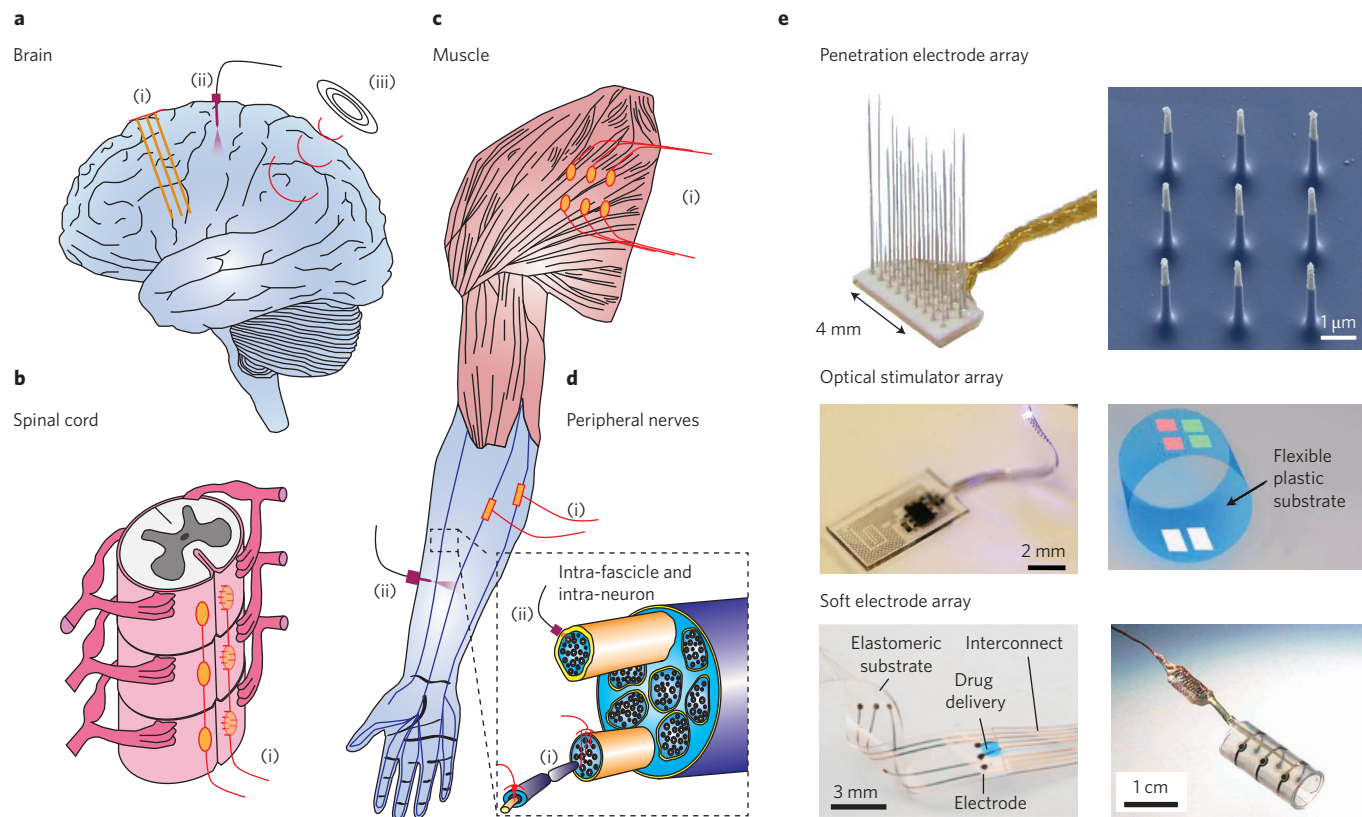


**Figure 6 | Emerging technologies with potential for interfacing nervous systems with information from prosthetic electronic skin. a–d**, Potential interfacing sites include the brain (**a**), spinal cord (**b**), muscle (**c**) and peripheral nerves (**d**). Potential interfacing approaches include electrical stimulation (i), optical stimulation (ii) and magnetic stimulation (iii). Inset: zoomed-in region of the dashed black box showing the potential interface of a few or individual neurons inside a fascicle through electrical stimulation (i) and optical stimulation (ii). **e**, Top: electrode array for stimulating intra-fascicular neural and intra-neuronal activity. Penetration electrode array<sup>128</sup> (left) and intracellular electrode array<sup>112</sup> (right). Middle: micro-light-emitting diode (LED) array for optogenetically evoked cell-specific activity. Stretchable LED<sup>118</sup> (left) and multi-coloured LED arrays<sup>129</sup> (right). Bottom: soft electronics for providing a long-term stable bio-electronic interface. Soft multifunctional electrode array<sup>119</sup> (left) and cuff electrodes<sup>106</sup> (right). Panel **e** reproduced with permission from: top left, ref. 128, Taylor & Francis; top right, middle left, middle right, refs 112,118,129, Nature Publishing Group; bottom left, ref. 119, AAAS; bottom right, ref. 106, Wiley.

is required to provoke nerve activities, which cannot produce discriminable sensations with high resolution.

For potential applications of prosthetic electronic skin, it is expected that highly dense sensor arrays and multiple types of sensors will be incorporated to imitate skin sensory functions. Therefore, to enhance localization and specification of stimulation for precise and discriminable perception restoration, electrodes that can target individual fascicles or even individual neurons are more attractive (Fig. 6d inset (i)). Recently, the integration of an artificial fingertip tactile sensor with transverse intra-fascicular multichannel electrodes implanted in a patient has been reported, aiming at targeting fewer neurons inside peripheral nerve fascicles<sup>109</sup>. Sensor outputs were converted into biomimetic signals by an external set-up to reflect the different tactile stimuli. Owing to the highly specific stimulation, the patient could distinguish the different textures touched by the fingertip sensor. To create highly localized and widely distributed percepts with distinct functional input, high-density intra-fascicular electrode arrays such as Utah slanted electrode arrays<sup>110</sup> or even nanowire intracellular electrodes (Fig. 6e, top)<sup>111</sup> could potentially be used to further localize the stimulated region for addressing individual axons within a distinct innervating area and function<sup>112</sup>.

**Optogenetic stimulation.** By introducing specific opsins (light-sensitive proteins) in targeted neurons of a primate's somatosensory cortex and triggering localized light stimuli in the brain, a sensation

can be reliably activated that the animal learns to interpret it as a tactile sensation localized within the hand<sup>113–115</sup> (Fig. 6a(ii)). Delivery of optical signals could be realized by using fibre-coupled lasers or flexible and multi-coloured arrays of light-emitting diodes (Fig. 6e, middle). Optogenetic methods are based on opsins that can be expressed only in specific types of cells. This is especially important in the restoration of touch perception directly into the CNS, in view of the complexity of neural coding in the CNS<sup>113–115</sup>. In addition, optogenetic stimulation can be more efficient and requires less complicated pulse waveforms compared with electrical stimulation, and as a result, the waveform conditioning circuitry could be simplified. Recently, full integration of a digital mechanoreceptor has been reported that could detect and convert *in situ* pressure signals from tactile sensors into biomimetic optical signals that stimulate somatosensory neurons with channelrhodopsin in mouse brain slices, showing the potential to directly input biomimetic touch signals in the brain through optogenetic stimulation<sup>92</sup>.

It has also recently been demonstrated that a transgenic rat expressing opsins in peripheral nerves could show a sensory-evoked behaviour in response to blue light flashes on the plantar skin (Fig. 6d(ii))<sup>116</sup>. In addition, optical nerve cuffs have been developed for chronic implantation with periphery nervous systems for optical stimulation, allowing cell-specific targeting in the nerve bundle (Fig. 6d inset (ii))<sup>117,118</sup>. However, although optogenetic approaches have provided a range of strategies to manipulate the activity of specific neural microcircuits and avoid artefacts typical

**Table 2 | Current methods for interfacing sensors for touch perception with the nervous system.**

	Electrical stimulation	Optical stimulation	Magnetic stimulation
Interface with central nervous system	Intracortical electrode <sup>101,102</sup> Epidural electrode <sup>97,104</sup>	Optical fibre <sup>113–115</sup> Micro-light-emitting diode <sup>118,120</sup>	Magnetic generator for transcranial magnetic stimulation <sup>13,100</sup>
Interface with peripheral nervous system	Surface electrode <sup>105</sup> Extra-fascicular electrode <sup>106,107</sup> Intra-fascicular electrode <sup>108,109</sup>	Surface light pulse <sup>116</sup> Optical nerve cuff <sup>117</sup>	Magnetic generator for transcutaneous magnetic stimulation <sup>13</sup>
Skin barrier	Surface electrode stimulating residual skin reinnervated by peripheral nerves <sup>105</sup>	Light pulse can penetrate skin for peripheral neuron stimulation	No skin barrier
Current stage for integration with sensor	Integration of a tactile sensor with intra-fascicular electrodes targeting human peripheral nerves to enable texture discrimination <sup>109</sup>	Integration of organic digital mechanoreceptor with fibre optics targeting somatosensory neurons in brain slices of mice <sup>92</sup>	N/A
Pros	Clinically applicable on human subjects	Cell-specific stimulation High stimulation efficiency	Wireless and non-invasive stimulation
Cons	Lack of specificity Low stimulation efficiency	Regulatory issues for clinical trials with human patients	No specificity Low stimulation resolution and efficiency

of electrical stimulation, due to the technical and regulatory hurdles in using genetic therapies in humans, their translation into clinical applications is still non-trivial compared with electrical methods<sup>98</sup>.

**Magnetic stimulation.** Transcranial and transcutaneous magnetic stimulations have been studied for tactile sensing applications (Fig. 6a(iii)). Magnetic stimulation employs coils, which could be implemented into the prosthetic electronic skin devices as surface magnetic generators in contact with the skin. The coil generates a magnetic field that easily penetrates the skin barrier and induces an electric current that activates the neurons. These methods are advantageous because of their non-invasiveness; yet, they are currently limited by poor resolution, lack of specificity and low stimulation efficiency<sup>13</sup>. As an alternative approach, magnetic field energy is translated into thermal energy that controls neural excitation in a minimally invasive manner, through the activation of the heat-sensitive capsaicin receptor TRPV1 functionalized with magnetic nanoparticles<sup>100</sup>. This provides a method for remote control of specific neuron activity; however, the spatiotemporal resolution and possibility of clinical application need to be further investigated.

**Chronic and wireless interfacing with nerve system.** The chronic stability and robustness against patient motion of the interface between the central or peripheral nervous systems and the implanted electrodes or optical devices is a critical aspect for prosthetic skin. Currently, soft electronics designs have been demonstrated to provide a stable chronic interface with nervous systems (Fig. 6e, bottom). These allow the implanted electronics to have mechanical properties similar to the nervous system and to reduce both chronic damage to neurons and scar tissue formation around the electronics<sup>119–121</sup>. Soft electronics for both electrical and optical modulation of the nervous system have been developed. Alternatively, wireless implanted electronics have also been demonstrated for interfacing with the central and peripheral nervous systems in freely behaving animals<sup>118,120,122</sup>.

### Perspective

The challenge of creating prosthetic electronic skin is multifaceted and requires advancements in many fields, including mechanically compliant electronics, transducers, neural interfaces and associated materials and devices. Some technologies, such as transducers, flexible electronics and stretchable electronics based on traditional electronic materials, have reached sufficient maturity to start producing integrated prototypes<sup>75,92</sup>. Several of the key demonstrations are

highlighted in Table 1. Each technology platform has reached different levels of sophistication. Rigid silicon can provide comparable device densities with highly conditioned output<sup>123</sup>. Silicon electronics has further been leveraged to create stretchable prosthetic skin with multifunctional capabilities<sup>75</sup>, but integrated signal processing has not yet been implemented. Flexible inorganic devices have been demonstrated with sensor densities much higher than real skin<sup>78</sup>, but lacked signal-conditioning capabilities. Emerging organic and carbon-based circuits have enabled flexible active matrix arrays with suitable sensor densities<sup>59,71</sup>, whereas devices with biomimetic electrical output have reached proof-of-concept stage<sup>92</sup>. Intrinsically stretchable systems have demonstrated simple passive matrix sensor arrays without active data acquisition<sup>89</sup>. Work towards improving the density and robustness of flexible devices includes the investigation of short channel devices<sup>124</sup>, complementary circuits<sup>31</sup> and the development of pseudo-CMOS<sup>32</sup> strategies for low-power, high-performance devices. One of the key issues will be the development of manufacturing techniques that enable large-area fabrication with low cost and high yield<sup>27</sup>, such as gravure printing<sup>71</sup> and inkjet printing<sup>92</sup>. Several proof-of-concept examples have demonstrated simple coverings for prosthetic hands composed of flexible tactile sensors or stretchable multifunctional sensor arrays, with an external set-up to convert biomimetic signals. Key issues for the design of a fully functional prosthetic electronic skin include the development of lightweight and wearable readout circuits, integration of circuits and sensors and testing and optimization of mechanical robustness, life-like feeling as well as aesthetic design. These challenges provide major motivation and opportunities for materials, devices and processing development. The other limiting factors in the field are currently the scarcity of stable neural interfaces, the limited number of input channels that the neural interfaces provide, and the limited understanding of neural coding.

An open question in the field is the extent to which sensor arrays for prosthetics should be biomimetic. Biological cutaneous sensors have characteristics that are often considered to be non-ideal<sup>12</sup>, because they are often sensitive to more than one stimulus, they have time-varying, hysteretic response, and some have limited accuracy. The biological sensory system overcomes these limitations through complex neural coding mechanisms and by recruiting information from a very large number of sensors (17,000 in one hand<sup>14</sup>) with overlapping receptive fields and target stimuli<sup>13,18</sup>. The use of artificial receptors with more ideal electrical characteristics may have advantages, but it is unclear whether sensors with non-ideal biomimetic characteristics such as hysteretic response would provide a more natural sensation.

Although the number of sensory signals that can be injected into the nervous system is currently limited, even a small number of sensors can substantially improve the utility of prosthetic devices<sup>90,110</sup>. To recover the ability to sense more complex stimuli such as surface textures and object shape, a large number of receptors is necessary. Emerging strategies for making electrical contact to individual neurons, including nanoscale intracellular electrodes and cell-specific optogenetic stimulation, provide a promising future to specifically inject signals from sensors in a high-density array to the corresponding peripheral nerve fibres (Fig. 6e). In addition, the progress of soft electronics shows substantial improvement for building chronically stable electrode–neuron interfacing, especially for interfacing with tissue subjected to frequent movement.

In the short term, biomimetic prosthetic electronic skin with a large density of sensors could be useful for advanced robotics, which can more easily make use of a large number of input signals. Combining biomimetic sensors<sup>123</sup> and neuromorphic sensor analysis<sup>125</sup> could result in tactile sensor systems with very low power consumption, similar to low-power vision systems provided by artificial retinas<sup>126</sup>.

Received 25 January 2016; accepted 19 May 2016;  
published online 4 July 2016

## References

- Nghiem, B. T. *et al.* Providing a sense of touch to prosthetic hands. *Plast. Reconstr. Surg.* **135**, 1652–1663 (2015).
- Antfolk, C. *et al.* Sensory feedback in upper limb prosthetics. *Exp. Rev. Med. Dev.* **10**, 45–54 (2013).
- Marasco, P. D., Kim, K., Colgate, J. E., Peshkin, M. A. & Kuiken, T. A. Robotic touch shifts perception of embodiment to a prosthesis in targeted reinnervation amputees. *Brain* **134**, 747–758 (2011).
- Flor, H., Denke, C., Schaefer, M. & Grusser, S. Effect of sensory discrimination training on cortical reorganization and phantom limb pain. *Lancet* **357**, 1763–1764 (2001).
- Saal, H. P. & Bensmaia, S. J. Biomimetic approaches to bionic touch through a peripheral nerve interface. *Neuropsychologia* **79**, 344–353 (2015).
- Johansson, R. S. & Westling, G. Signals in tactile afferents from the fingers eliciting adaptive motor responses during precision grip. *Exp. Brain Res.* **66**, 141–154 (1987).
- Wijk, U. & Carlsson, I. Forearm amputees' views of prosthesis use and sensory feedback. *J. Hand Ther.* **28**, 269–278 (2015).
- Biddiss, E., Beaton, D. & Chau, T. Consumer design priorities for upper limb prosthetics. *Disabil. Rehabil. Assist. Technol.* **2**, 346–357 (2007).
- Campero, M., Serra, J., Bostock, H. & Ochoa, J. L. Slowly conducting afferents activated by innocuous low temperature in human skin. *J. Physiol.* **535**, 855–865 (2001).
- Campero, M. & Bostock, H. Unmyelinated afferents in humans and their responsiveness to low temperature. *Neurosci. Lett.* **470**, 188–192 (2010).
- Hensel, H. Thermoreceptors. *Annu. Rev. Physiol.* **36**, 233–249 (1974).
- Dahiya, R. S., Metta, G., Valle, M. & Sandini, G. Tactile sensing: from humans to humanoids. *IEEE Trans. Robotics* **26**, 1–20 (2010).
- Johansson, R. S. & Flanagan, J. R. Coding and use of tactile signals from the fingertips in object manipulation tasks. *Nature Rev. Neurosci.* **10**, 345–359 (2009).
- Abraira, V. E. & Ginty, D. D. The sensory neurons of touch. *Neuron* **79**, 618–639 (2013).
- Weber, A. I. *et al.* Spatial and temporal codes mediate the tactile perception of natural textures. *Proc. Natl Acad. Sci. USA* **110**, 17107–17112 (2013).
- Jenmalm, P., Birznieks, I., Goodwin, A. W. & Johansson, R. S. Influence of object shape on responses of human tactile afferents under conditions characteristic of manipulation. *Eur. J. Neurosci.* **18**, 164–176 (2003).
- Scheibert, J., Leurent, S., Prevost, A. & Debrégeas, G. The role of fingerprints in the coding of tactile information probed with a biomimetic sensor. *Science* **323**, 1503–1506 (2009).
- Johansson, R. S. & Birznieks, I. First spikes in ensembles of human tactile afferents code complex spatial fingertip events. *Nature Neurosci.* **7**, 170–177 (2004).
- Adams, M. J. *et al.* Finger pad friction and its role in grip and touch. *J. R. Soc. Interface* **10**, 20120467 (2013).
- Johansson, R. S. & Vallbo, A. B. Tactile sensibility in the human hand: relative and absolute densities of four types of mechanoreceptive units in glabrous skin. *J. Physiol.* **286**, 283–300 (1979).
- Tiest, W. M. B. Tactile perception of material properties. *Vision Res.* **50**, 2775–2782 (2010).
- Ackerley, R., Olausson, H., Wessberg, J. & McGlone, F. Wetness perception across body sites. *Neurosci. Lett.* **522**, 73–77 (2012).
- Hammock, M. L., Chortos, A., Tee, B. C. K., Tok, J. B. H. & Bao, Z. 25th anniversary article: the evolution of electronic skin (e-skin): a brief history, design considerations, and recent progress. *Adv. Mater.* **25**, 5997–6038 (2013).
- Lumelsky, V. J., Shur, M. S. & Wagner, S. Sensitive skin. *IEEE Sens. J.* **1**, 41–51 (2001).
- Rogers, J. A., Someya, T. & Huang, Y. Materials and mechanics for stretchable electronics. *Science* **327**, 1603–1607 (2010).
- Cabibihan, J. J., Joshi, D., Srinivasa, Y. M., Chan, M. A. & Muruganatham, A. Illusory sense of human touch from a warm and soft artificial hand. *IEEE Trans. Neural Syst. Rehab. Eng.* **23**, 517–527 (2015).
- Khan, S., Lorenzelli, L. & Dahiya, R. S. Technologies for printing sensors and electronics over large flexible substrates: a review. *IEEE Sens. J.* **15**, 3164–3185 (2015).
- Wong, W. S. & Salleo, A. *Flexible Electronics* (Springer Science Business Media, 2009).
- Takei, K. *et al.* Nanowire active-matrix circuitry for low-voltage macroscale artificial skin. *Nature Mater.* **9**, 821–826 (2010).
- Kim, K. *et al.* Polymer-based flexible tactile sensor up to 32 × 32 arrays integrated with interconnection terminals. *Sens. Actuat. A* **156**, 284–291 (2009).
- Chen, H., Cao, Y., Zhang, J. & Zhou, C. Large-scale complementary macroelectronics using hybrid integration of carbon nanotubes and IGZO thin-film transistors. *Nature Commun.* **5**, 4097 (2014).
- Yokota, T. *et al.* Sheet-type flexible organic active matrix amplifier system using pseudo-CMOS circuits with floating-gate structure. *IEEE Trans. Electron Dev.* **59**, 3434–3441 (2012).
- Kaltenbrunner, M. *et al.* An ultra-lightweight design for imperceptible plastic electronics. *Nature* **499**, 458–463 (2013).
- Edwards, C. & Marks, R. Evaluation of biomechanical properties of human skin. *Clin. Dermatol.* **13**, 375–380 (1995).
- Yamada, T. *et al.* A stretchable carbon nanotube strain sensor for human-motion detection. *Nature Nanotech.* **6**, 296–301 (2011).
- Harris, K. D., Elias, A. L. & Chung, H.-J. Flexible electronics under strain: a review of mechanical characterization and durability enhancement strategies. *J. Mater. Sci.* **51**, 2771–2805 (2015).
- Kim, D.-H. *et al.* Stretchable and foldable silicon integrated circuits. *Science* **320**, 507–511 (2008).
- Schwartz, G. *et al.* Flexible polymer transistors with high pressure sensitivity for application in electronic skin and health monitoring. *Nature Commun.* **4**, 1859 (2013).
- Kim, D.-H. *et al.* Materials and noncoplanar mesh designs for integrated circuits with linear elastic responses to extreme mechanical deformations. *Proc. Natl Acad. Sci. USA* **105**, 18675–18680 (2008).
- Sekitani, T. *et al.* A rubberlike stretchable active matrix using elastic conductors. *Science* **321**, 1468–1472 (2008).
- Benight, S. J., Wang, C., Tok, J. B. H. & Bao, Z. Stretchable and self-healing polymers and devices for electronic skin. *Prog. Polym. Sci.* **38**, 1961–1977 (2013).
- O'Connor, T. F., Rajan, K. M., Printz, A. D. & Lipomi, D. J. Toward organic electronics with properties inspired by biological tissue. *J. Mater. Chem. B* **3**, 4947–4952 (2015).
- Chun, K.-Y. *et al.* Highly conductive, printable and stretchable composite films of carbon nanotubes and silver. *Nature Nanotech.* **5**, 853–857 (2010).
- Lipomi, D. J. *et al.* Skin-like pressure and strain sensors based on transparent elastic films of carbon nanotubes. *Nature Nanotech.* **6**, 788–792 (2011).
- Chortos, A. *et al.* Mechanically durable and highly stretchable transistors employing carbon nanotube semiconductor and electrodes. *Adv. Mater.* **28**, 4441–4448 (2016).
- Yun, S. *et al.* Compliant silver nanowire–polymer composite electrodes for bistable large strain actuation. *Adv. Mater.* **24**, 1321–1327 (2012).
- Savagatrup, S., Printz, A. D., O'Connor, T., Zaretski, A. V. & Lipomi, D. J. Molarly stretchable electronics. *Chem. Mater.* **26**, 3028–3041 (2014).
- Lipomi, D. J. *et al.* Electronic properties of transparent conductive films of PEDOT:PSS on stretchable substrates. *Chem. Mater.* **24**, 373–382 (2012).
- Trung, T. Q., Ramasundaram, S., Hwang, B.-U. & Lee, N.-E. An all-elastomeric transparent and stretchable temperature sensor for body-attachable wearable electronics. *Adv. Mater.* **28**, 502–509 (2015).
- Park, S. *et al.* Stretchable energy-harvesting tactile electronic skin capable of differentiating multiple mechanical stimuli modes. *Adv. Mater.* **26**, 7324–7332 (2014).
- Choong, C.-L. *et al.* Highly stretchable resistive pressure sensors using a conductive elastomeric composite on a micropyramid array. *Adv. Mater.* **26**, 3451–3458 (2014).

52. Hu, W., Niu, X., Zhao, R. & Pei, Q. Elastomeric transparent capacitive sensors based on an interpenetrating composite of silver nanowires and polyurethane. *Appl. Phys. Lett.* **102**, 083303 (2013).
53. Shin, M. *et al.* Highly stretchable polymer transistors consisting entirely of stretchable device components. *Adv. Mater.* **26**, 3706–3711 (2014).
54. Sekiguchi, A. *et al.* Robust and soft elastomeric electronics tolerant to our daily lives. *Nano Lett.* **15**, 5716–5723 (2015).
55. de Boissieu, F. *et al.* Tactile texture recognition with a 3-axial force MEMS integrated artificial finger. In *Proc. Robotics: Science and Systems* 49–56 (MIT Press, 2009).
56. Jang, K.-I. *et al.* Soft network composite materials with deterministic and bio-inspired designs. *Nature Commun.* **6**, 6566 (2015).
57. Dykes, R. W. Coding of steady and transient temperatures by cutaneous 'cold' fibers serving the hand of monkeys. *Brain Res.* **98**, 485–500 (1975).
58. Webb, R. C. *et al.* Ultrathin conformal devices for precise and continuous thermal characterization of human skin. *Nature Mater.* **12**, 938–944 (2013).
59. Someya, T. *et al.* Conformable, flexible, large-area networks of pressure and thermal sensors with organic transistor active matrixes. *Proc. Natl Acad. Sci. USA* **102**, 12321–12325 (2005).
60. Yokota, T. *et al.* Ultraflexible, large-area, physiological temperature sensors for multipoint measurements. *Proc. Natl Acad. Sci. USA* **112**, 14533–14538 (2015).
61. Jeon, J., Lee, H.-B.-R. & Bao, Z. Flexible wireless temperature sensors based on Ni microparticle-filled binary polymer composites. *Adv. Mater.* **25**, 850–855 (2013).
62. Edin, B. B., Essick, G. K., Trulsson, M. & Olsson, K. A. Receptor encoding of moving tactile stimuli in humans. I. Temporal pattern of discharge of individual low-threshold mechanoreceptors. *J. Neurosci.* **15**, 830–847 (1995).
63. Ge, W. & Khalsa, P. S. Encoding of compressive stress during indentation by slowly adapting type I mechanoreceptors in rat hairy skin. *J. Neurophysiol.* **87**, 1686–1693 (2002).
64. Burgess, P. R. *et al.* The neural signal for skin indentation depth. I. Changing indentations. *J. Neurosci.* **3**, 1572–1585 (1983).
65. Mannsfeld, S. C. B. *et al.* Highly sensitive flexible pressure sensors with microstructured rubber dielectric layers. *Nature Mater.* **9**, 859–864 (2010).
66. Zang, Y. *et al.* Flexible suspended gate organic thin-film transistors for ultra-sensitive pressure detection. *Nature Commun.* **6**, 6269 (2015).
67. Tee, B. C. K., Wang, C., Allen, R. & Bao, Z. An electrically and mechanically self-healing composite with pressure- and flexion-sensitive properties for electronic skin applications. *Nature Nanotech.* **7**, 825–832 (2012).
68. Pan, L. *et al.* An ultra-sensitive resistive pressure sensor based on hollow-sphere microstructure induced elasticity in conducting polymer film. *Nature Commun.* **5**, 3002 (2014).
69. Lee, S. *et al.* A transparent bending-insensitive pressure sensor. *Nature Nanotech.* **11**, 472–478 (2016).
70. Boutry, C. M. *et al.* A sensitive and biodegradable pressure sensor array for cardiovascular monitoring. *Adv. Mater.* **27**, 6954–6961 (2015).
71. Yeom, C. *et al.* Large-area compliant tactile sensors using printed carbon nanotube active-matrix backplanes. *Adv. Mater.* **27**, 1561–1566 (2015).
72. Chossat, J.-B., Park, Y.-L. & Wood, R. J. A soft strain sensor based on ionic and metal liquids. *IEEE Sens. J.* **13**, 3405–3414 (2013).
73. Kanda, Y. Piezoresistance effect of silicon. *Sens. Actuat. A* **28**, 83–91 (1991).
74. Hu, N., Karube, Y., Yan, C., Masuda, Z. & Fukunaga, H. Tunneling effect in a polymer/carbon nanotube nanocomposite strain sensor. *Acta Mater.* **56**, 2929–2936 (2008).
75. Kim, J. *et al.* Stretchable silicon nanoribbon electronics for skin prosthesis. *Nature Commun.* **5**, 5747 (2014).
76. Park, Y.-L., Majidi, C., Kramer, R., Bérard, P. & Wood, R. J. Hyperelastic pressure sensing with a liquid-embedded elastomer. *J. Micromech. Microeng.* **20**, 125029 (2010).
77. Broadhurst, M. G., Davis, G. T. & McKinney, J. E. Piezoelectricity and pyroelectricity in polyvinylidene fluoride — a model. *J. Appl. Phys.* **49**, 4992–4997 (1978).
78. Wu, W., Wen, X. & Wang, Z. L. Taxel-addressable matrix of vertical-nanowire piezotronic transistors for active and adaptive tactile imaging. *Science* **340**, 952–957 (2013).
79. Tien, N. T. *et al.* A flexible bimodal sensor array for simultaneous sensing of pressure and temperature. *Adv. Mater.* **26**, 796–804 (2014).
80. Wang, Z. L., Chen, J. & Lin, L. Progress in triboelectric nanogenerators as a new energy technology and self-powered sensors. *Energy Environ. Sci.* **8**, 2250–2282 (2015).
81. Persano, L. *et al.* High performance piezoelectric devices based on aligned arrays of nanofibers of poly(vinylidene fluoride-co-trifluoroethylene). *Nature Commun.* **4**, 1633 (2013).
82. Qi, Y. *et al.* Enhanced piezoelectricity and stretchability in energy harvesting devices fabricated from buckled PZT ribbons. *Nano Lett.* **11**, 1331–1336 (2011).
83. Park, J., Kim, M., Lee, Y., Lee, H. S. & Ko, H. Fingertip skin-inspired microstructured ferroelectric skins discriminate static/dynamic pressure and temperature stimuli. *Sci. Adv.* **1**, e1500661 (2015).
84. Jung, Y., Lee, D.-G., Park, J., Ko, H. & Lim, H. Piezoresistive tactile sensor discriminating multidirectional forces. *Sensors* **15**, 25463–25473 (2015).
85. Aoyagi, S., Tanaka, T. & Minami, M. Recognition of contact state of four layers arrayed type tactile sensor by using neural network. In *IEEE Int. Conf. Information Acquisition* 393–397 (IEEE, 2006).
86. Schmitz, A., Maggiali, M., Randazzo, M., Natale, L. & Metta, G. A prototype fingertip with high spatial resolution pressure sensing for the robot iCub. In *IEEE-RAS Int. Conf. Humanoid Robots* 423–428 (IEEE, 2008).
87. Shimojo, M. Spatial filtering characteristic of elastic cover for tactile sensor. In *IEEE Int. Conf. Robotics and Automation* 287–292 (IEEE, 1994).
88. Graz, I. *et al.* Flexible active-matrix cells with selectively poled bifunctional polymer-ceramic nanocomposite for pressure and temperature sensing skin. *J. Appl. Phys.* **106**, 034503 (2009).
89. Ho, D. H. *et al.* Stretchable and multimodal all graphene electronic skin. *Adv. Mater.* **28**, 2601–2608 (2016).
90. Tan, D. W. *et al.* A neural interface provides long-term stable natural touch perception. *Sci. Transl. Med.* **6**, 257ra138 (2014).
91. Viventi, J. *et al.* A conformal, bio-interfaced class of silicon electronics for mapping cardiac electrophysiology. *Sci. Transl. Med.* **2**, 24ra22 (2010).
92. Tee, B. C.-K. *et al.* A skin-inspired organic digital mechanoreceptor. *Science* **350**, 313–316 (2015).
93. Nag, S., Xiaofeng, J., Thakor, N. & Sharma, D. Flexible charge balanced stimulator with 5.6 fC accuracy for 140 nC injections. *IEEE Trans. Biomed. Circuits Syst.* **7**, 266–275 (2013).
94. Chen, L. Y. *et al.* Continuous wireless pressure monitoring and mapping with ultra-small passive sensors for health monitoring and critical care. *Nature Commun.* **5**, 5028 (2014).
95. Xu, S. *et al.* Soft microfluidic assemblies of sensors, circuits, and radios for the skin. *Science* **344**, 70–74 (2014).
96. Mohammadi, A., Yuce, M. R. & Moheimani, S. O. R. Frequency modulation technique for MEMS resistive sensing. *IEEE Sens. J.* **12**, 2690–2698 (2012).
97. Borton, D., Micera, S., Millán, J. d. R. & Courtine, G. Personalized neuroprosthetics. *Sci. Transl. Med.* **5**, 210rv212 (2013).
98. Chow, B. Y. & Boyden, E. S. Optogenetics and translational medicine. *Sci. Transl. Med.* **5**, 177ps175 (2013).
99. Tufail, Y. *et al.* Transcranial pulsed ultrasound stimulates intact brain circuits. *Neuron* **66**, 681–694 (2010).
100. Chen, R., Romero, G., Christiansen, M. G., Mohr, A. & Anikeeva, P. Wireless magnetothermal deep brain stimulation. *Science* **347**, 1477–1480 (2015).
101. Tabot, G. A. *et al.* Restoring the sense of touch with a prosthetic hand through a brain interface. *Proc. Natl Acad. Sci. USA* **110**, 18279–18284 (2013).
102. Bensmaia, S. J. & Miller, L. E. Restoring sensorimotor function through intracortical interfaces: progress and looming challenges. *Nature Rev. Neurosci.* **15**, 313–325 (2014).
103. Li, L. *et al.* The functional organization of cutaneous low-threshold mechanosensory neurons. *Cell* **147**, 1615–1627 (2011).
104. van den Brand, R. *et al.* Restoring voluntary control of locomotion after paralyzing spinal cord injury. *Science* **336**, 1182–1185 (2012).
105. Kuiken, T. A., Marasco, P. D., Lock, B. A., Harden, R. N. & Dewald, J. P. A. Redirection of cutaneous sensation from the hand to the chest skin of human amputees with targeted reinnervation. *Proc. Natl Acad. Sci. USA* **104**, 20061–20066 (2007).
106. Hassler, C., Boretius, T. & Stieglitz, T. Polymers for neural implants. *J. Polym. Sci. B: Polym. Phys.* **49**, 18–33 (2011).
107. Tyler, D. J. & Durand, D. M. Functionally selective peripheral nerve stimulation with a flat interface nerve electrode. *IEEE Trans. Neural Syst. Rehab. Eng.* **10**, 294–303 (2002).
108. Raspopovic, S. *et al.* Restoring natural sensory feedback in real-time bidirectional hand prostheses. *Sci. Transl. Med.* **6**, 222ra219 (2014).
109. Oddo, C. M. *et al.* Intranural stimulation elicits discrimination of textural features by artificial fingertip in intact and amputee humans. *eLife* **5**, e09148 (2016).
110. Clark, G. A. *et al.* Using multiple high-count electrode arrays in human median and ulnar nerves to restore sensorimotor function after previous transradial amputation of the hand. In *Conf. Proc. IEEE Eng. Med. Biol. Soc.* 1977–1980 (IEEE, 2014).
111. Spira, M. E. & Hai, A. Multi-electrode array technologies for neuroscience and cardiology. *Nature Nanotech.* **8**, 83–94 (2013).
112. Robinson, J. T. *et al.* Vertical nanowire electrode arrays as a scalable platform for intracellular interfacing to neuronal circuits. *Nature Nanotech.* **7**, 180–184 (2012).
113. Huber, D. *et al.* Sparse optical microstimulation in barrel cortex drives learned behaviour in freely moving mice. *Nature* **451**, 61–64 (2008).

114. O'Connor, D. H. *et al.* Neural coding during active somatosensation revealed using illusory touch. *Nature Neurosci.* **16**, 958–965 (2013).
115. May, T. *et al.* Detection of optogenetic stimulation in somatosensory cortex by non-human primates — towards artificial tactile sensation. *PLoS ONE* **9**, e114529 (2014).
116. Ji, Z.-G. *et al.* Light-evoked somatosensory perception of transgenic rats that express channelrhodopsin-2 in dorsal root ganglion cells. *PLoS ONE* **7**, e32699 (2012).
117. Towne, C., Montgomery, K. L., Iyer, S. M., Deisseroth, K. & Delp, S. L. Optogenetic control of targeted peripheral axons in freely moving animals. *PLoS ONE* **8**, e72691 (2013).
118. Park, S. I. *et al.* Soft, stretchable, fully implantable miniaturized optoelectronic systems for wireless optogenetics. *Nature Biotechnol.* **33**, 1280–1286 (2015).
119. Mineev, I. R. *et al.* Electronic dura mater for long-term multimodal neural interfaces. *Science* **347**, 159–163 (2015).
120. Kim, T.-i. *et al.* Injectable, cellular-scale optoelectronics with applications for wireless optogenetics. *Science* **340**, 211–216 (2013).
121. Liu, J. *et al.* Syringe-injectable electronics. *Nature Nanotech.* **10**, 629–636 (2015).
122. Ho, J. S. *et al.* Wireless power transfer to deep-tissue microimplants. *Proc. Natl Acad. Sci. USA* **111**, 7974–7979 (2014).
123. Dahiya, R. S. *et al.* Tactile sensing chips with POSFET array and integrated interface electronics. *IEEE Sens. J.* **14**, 3448–3457 (2014).
124. Kraft, U. *et al.* Flexible low-voltage organic complementart circuits: finding the optimum combination of semiconductors and monolayer gate dielectrics. *Adv. Mater.* **27**, 207–214 (2015).
125. Lee, W. W., Kukreja, S. L. & Thakor, N. V. A kilohertz kilotaxel tactile sensor array for investigating spatiotemporal features in neuromorphic touch. In *IEEE Biomed. Circuits Syst. Conf.* 1–4 (IEEE, 2015).
126. Liu, S.-C. & Delbruck, T. Neuromorphic sensory systems. *Curr. Opin. Neurobiol.* **20**, 288–295 (2010).
127. Fan, F. R. *et al.* Transparent triboelectric nanogenerators and self-powered pressure sensors based on micropatterned plastic films. *Nano Lett.* **12**, 3109–3114 (2012).
128. Weber, D. J., Friesen, R. & Miller, L. E. Interfacing the somatosensory system to restore touch and proprioception: essential considerations. *J. Motor Behav.* **44**, 403–418 (2012).
129. Lochner, C. M., Khan, Y., Pierre, A. & Arias, A. C. All-organic optoelectronic sensor for pulse oximetry. *Nature Commun.* **5**, 5745 (2014).

### Acknowledgements

We acknowledge the support from Samsung Electronics, the MSIP (Ministry of Science, ICT and Future Planning), Korea, under the IT Consilience Creative Program (grant NIPA-2014-H0201-14-1001) supervised by the National IT Industry Promotion Agency and Air Force Office of Scientific Research (grant no. FA9550-15-1-0106).

### Author contributions

A.C., J.L. and Z.B. co-wrote the paper.

### Additional information

Reprints and permissions information is available at [www.nature.com/reprints](http://www.nature.com/reprints). Correspondence requests for materials should be addressed to Z.B.

### Competing financial interests

The authors declare no competing financial interests.